



Study of GaN:Eu³⁺ Thin Films Deposited by Metallorganic Vapor-Phase Epitaxy

J. Laski,^a K. Klinedinst, M. Raukas,^{a,*} K. C. Mishra,^{a,*z} J. Tao,^b J. McKittrick,^b
and J. B. Talbot^{b,**}

^aOSRAM SYLVANIA, Central Research, Beverly, Massachusetts 01915, USA

^bMaterials Science and Engineering Program, University of California, San Diego,
La Jolla, California 92093, USA

Using metallorganic vapor-phase epitaxy, thin films of gallium nitride activated by Eu³⁺ (GaN:Eu³⁺) have been deposited on sapphire substrates at atmospheric pressure. Luminescence from Eu³⁺ ions in GaN has been investigated using photoluminescence (PL) and PL excitation spectroscopy. Experimental results show that Eu³⁺ ions are excited via energy transfer from the host. Analyses of the observed emission and excitation spectra indicate occupancy of multiple sites in the nitride lattice. Using a pulsed laser source, variation of emission intensity with increasing excitation intensity has also been examined. The possibility of emission saturation at high excitation intensity is discussed from the perspective of application in light-emitting diode sources. © 2008 The Electrochemical Society. [DOI: 10.1149/1.2969910] All rights reserved.

Manuscript submitted March 21, 2008; revised manuscript received July 22, 2008. Published September 22, 2008.

During the last decade, there have been considerable research efforts for developing luminescent materials using III-V nitride hosts activated by trivalent rare-earth ions, RE³⁺.¹⁻¹⁰ Thin films of such materials have potential for use as active layers in nitride-based optoelectronic devices. Emissions from RE³⁺ ions originating from the f → f intraconfigurational transitions are weakly dependent on the host lattice. It is for this reason that the fluorescent materials are often designed using RE³⁺ ions in oxide hosts for lighting applications.¹¹ For example, the red emission from Eu³⁺ due to ⁵D₀ → ⁷F₂ transition near 612 nm and green emission from Tb³⁺ transition ⁵D₄ → ⁷F₅ transitions near 545 nm in oxide phosphors are often used as red and green components for generating white light in fluorescent lighting in combination with a broadband blue emission from a divalent europium ion due to 5d → 4f transition. Narrowband emissions from 4f → 4f transitions of RE³⁺ accompanied by their relative insensitiveness to the host lattice provide an effective tool for color blending. In this paper, we have analyzed the origin and characteristics of red emission due to the ⁵D₀ → ⁷F₂ transition of Eu³⁺ ions in GaN thin films deposited by metallorganic vapor-phase epitaxy (MOVPE).

Developing fluorescent materials using GaN, AlN, InN, and their alloys as hosts and RE³⁺ ions as activators will be a great stride toward an integrated optoelectronics device. A double heterojunction using such a material as the active layer could generate the white light within the device itself compared to a hybrid unit in which bandedge or excitonic emission is converted to white light by an external phosphor layer. Such a design could eliminate several loss processes and thereby improve the overall efficacy of a light-emitting diode (LED) based lighting system.

During the last few years, there have been many successful attempts demonstrating emission from RE³⁺ ions in AlN and GaN hosts. In powder samples, emission from Tm³⁺, Eu³⁺, Tb³⁺, Dy³⁺, and Er³⁺ has been demonstrated in GaN and AlN hosts by us and others.¹²⁻¹⁵ Thin films of nitrides activated by RE³⁺ have been prepared mostly by molecular beam epitaxy (MBE) or ion implantation of epilayers. Incorporation of RE³⁺ ions into nitride thin films by MOVPE has been thus far limited to Eu³⁺, Tb³⁺, and Er³⁺ ions.^{10,16,17} Because MOVPE deposition of GaN films is the method of choice for manufacturing, for this technology to be integrated to standard LED devices it is critical that this approach be thoroughly investigated and critical parameters for film deposition be established.

Although doping GaN and AlN thin films with RE³⁺ have been

demonstrated by a variety of techniques,¹⁻⁹ using MOVPE for this purpose continues to be a challenging process. There are several reasons that limited this approach for epitaxial thin-film deposition. First, there is only a small number of metallorganic precursors for this purpose. Second, the low vapor pressure of such materials requires transporting the metallorganic vapor to the reaction chamber at a high temperature. A typical MOVPE reactor must be modified extensively to transport vapors of these materials to the reaction chamber. Third, the long organic chains of these precursors are claimed to hinder the quality of GaN growth.¹⁸ Fourth, oxygen ligands of rare-earth ions in some metallorganic complexes could be a source for oxygen defects. Substitutional oxygen defects, such as O_N, are known to lower internal quantum efficiency and lead to unwanted emission from the defects on being excited near the bandedge.¹⁹ Finally, multiple valence states of rare-earth ions could impose additional restrictions for incorporation of RE³⁺ in the desired valence state. For example, europium ions normally exist in a trivalent or divalent state in a crystalline solid. For incorporating trivalent europium ions, oxidizing conditions are necessary, whereas normal deposition of GaN occurs in a reducing environment. Thus, ammonia to gallium flow rates must be controlled for doping GaN with trivalent europium ions. To the best of our knowledge, Pan and Steckl¹⁰ were the first and only to report deposition of GaN films with Eu³⁺ by in situ MOVPE, which showed characteristic red emission due to ⁵D₀ → ⁷F₂ transition.

In this paper, we report deposition of GaN:Eu³⁺ thin films by a MOVPE approach and spectroscopic and material characterization of these films. Additionally, site distribution of Eu³⁺ ions in the GaN lattice, the underlying mechanism of excitation, and the possibility of saturation of emission were investigated, which are relevant for lighting applications.

Experimental

Epitaxial growth of GaN:Eu³⁺ was carried out using a horizontal reactor designed for this purpose. Trimethylgallium (TMGa) and ammonia, NH₃, were used as the sources for Ga and N, respectively. In situ europium doping was performed using tris(2,2,6,6-tetramethyl-3,5-heptanedionato)europium, often referred to as Eu(TMHD)₃. TMGa has a reported melting point of -16°C and was used here in a bubbler heated to -15°C. Eu(TMHD)₃ has a reported melting point of 188°C but was sublimated in a standard bubbler at 135°C. The Eu(TMHD)₃ delivery lines were heated to an excess of 150°C to avoid condensation en route to the reaction chamber. The thin-film growth was carried out at atmospheric pressure (0.106 MPa) in contrast to Pan and Steckl¹⁰ where a 50 mTorr (6.7 Pa) pressure was maintained.

The thin films were grown on a sapphire substrate along the [0001] direction. The approximate growth rate of undoped GaN lay-

* Electrochemical Society Active Member.

** Electrochemical Society Fellow.

^z E-mail: kailash.mishra@sylvania.com

ers in our reactor is 1.2 $\mu\text{m}/\text{h}$. The growth rate of the GaN:Eu³⁺ layer was not measured explicitly, but was most likely similar, to the extent that Ga flux was assumed to be the limiting factor.

The entire deposition process consisted of the following steps:

1. Treatment of the sapphire substrate with 1 standard liters per minute (SLM) of H₂ at 1050°C for 10 min.
2. Nitridation of the sapphire substrate with a mixture of 1 SLM H₂ and 1.2 SLM NH₃ at 600°C for 60 s.
3. Deposition of ~20 nm thick GaN buffer layer at 600°C (using the above H₂/NH₃ mixture plus 2.4 sccm of H₂ carrier gas through the TMGa bubbler for 90 s).
4. Deposition of 1.2 μm of undoped GaN at 1030°C (using a mixture of 840 sccm H₂ push gas, 1.4 SLM NH₃, and 4 sccm of H₂ carrier gas through the TMGa bubbler for 60 min).
5. Deposition of GaN:Eu³⁺ at 1030°C for 60 min (a mixture of 840 sccm H₂ push gas, 15 sccm NH₃, 4 sccm of H₂ carrier gas through the TMGa bubbler, and 400 sccm of H₂ carrier gas through the Eu(TMHD)₃ sublimator).

The reactor was configured such that the Eu precursor-containing carrier gas merged with the other process gases (NH₃, TMGa, and H₂ push gas) at the final stage just before entering the reactor chamber. To reduce the chances of cooling the Eu precursor carrier gas to the point of condensation, these other gases were preheated to 90°C (an upper limit for our manifold valves). The pipe-fitting forming the junction, where these two sets of gases merge, was heated to 185°C in an attempt to compensate for this gas-temperature mismatch. Separate experiments that replace the quartz reactor chamber with a condensing-tube-trapped Eu(TMHD)₃ precursor at a rate of 0.09 micromoles/min (as measured using inductively coupled plasma emission spectroscopy) at flow rates through the bubbler of 200 sccm, which extrapolated to a rate of 0.18 micromoles/min at 400 sccm for our experiments, assuming linearity. This was within a factor of two of transport rates predicted from published reports of Eu(TMHD)₃ vapor pressure data.

There are several important aspects of the deposition process, that need further discussion. The source for Eu, Eu(TMHD)₃ has europium ions coordinated to oxygen-containing ligands. However, the thin films did not show any unexpected enhancement of oxygen concentration by energy dispersive X-ray spectroscopy (EDS) nor the blue band associated with increasing substitutional oxygen defects. We believe that the Eu(TMHD)₃ did not mix thoroughly with TMGa and NH₃ because the films typically show a gradient of europium concentration, [Eu], across the film that is highest on the same side as the entrance port for the precursor containing the gas stream. Physical mixing of the process gases to overcome this uniformity issue was not attempted in this work.

The EDS measurements showed that [Eu] varied from 0.1 to 0.5 at % from spot measurements of area ~0.01 mm. Two samples, F05252007 and F06082007, used in this study for spectroscopic measurements, varied in H₂-push gas flow, the former using only 150 sccm instead of 840 sccm mentioned earlier. The significance of this change on spatial distribution of Eu³⁺ ions was not quite obvious, although several differences with respect to site occupancy of these ions in the two films were noted from the spectroscopic measurements. The emission intensity from Eu³⁺ was observed to increase with increasing [Eu]. X-Ray diffraction (XRD) patterns showed growth along [0001] direction with weak 100 and 101 diffraction peaks corresponding to growth along the [10 $\bar{1}$ 0] and [10 $\bar{1}$ 1] directions.

Spectroscopic measurements were performed at room temperature using a 450 W Xe-lamp and pair of double monochromators (SPEX Fluorolog-2) or employing an optical parametric oscillator (OPO NT342-UV, Ekspla) as an excitation source and a 0.5 m monochromator with a cooled photomultiplier tube for detection.

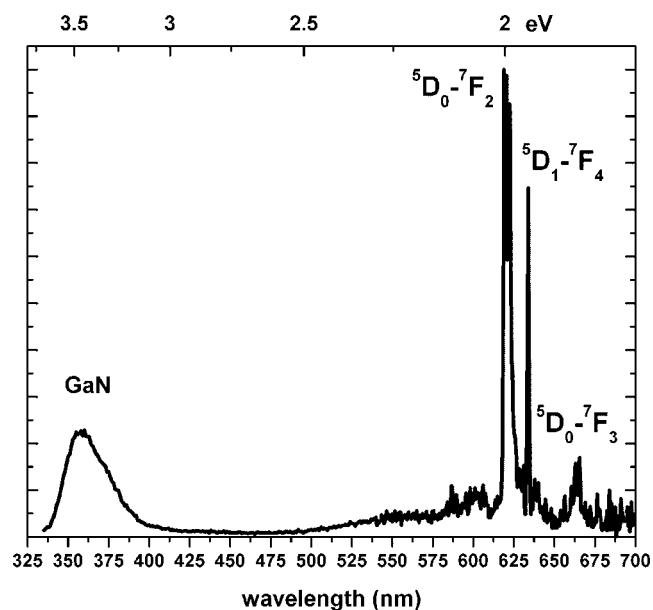


Figure 1. Room-temperature PL spectrum of GaN:Eu³⁺ thin film in response to lamp excitation at 300–330 nm.

Results

Several thin films prepared using the above approach were investigated by luminescence techniques. Photoluminescence (PL) and PL excitation (PLE) spectra from most films yielded similar features. The results presented here are from two samples having the highest [Eu] of about 0.1–0.5% as determined using the EDS measurements. Similar to other thin films prepared in the reactor, these films exhibited higher [Eu] near the substrate edge on the inlet side of the vaporized rare-earth precursors. However, the spatial resolution for luminescence measurements did not allow us to probe regions having different Eu³⁺ concentrations as observed from the EDS measurements. Typical PL and PLE spectra reported in this work describe the average response of Eu³⁺ ions over a region having the highest but spatially nonuniform Eu³⁺ concentrations.

Figure 1 shows the PL spectrum for lamp excitation in the 300–330 nm wavelength region. The emission yields strong, narrowband transitions in the red at approximately 619, 622, 634, 663, and 665 nm due to Eu³⁺, in addition to the GaN near-band-edge (NBE) luminescence around 360 nm. Though weak, the yellow emission band due to defects can be easily noted. The integrated strength of the Eu³⁺ emission peaks is comparable to that of GaN emission near 360 nm and supports the conjecture that electron-hole (e-h) pairs generated on excitation at energies equal to or greater than the bandgap are likely to recombine at Eu³⁺.

The sharp peaks observed at 621–622 nm have been assigned to the ⁵D₀ → ⁷F₂ transition of Eu³⁺ in the nitride environment in GaN¹⁰ and AlN.²⁰ However, various other wavelength values have also been reported depending on the method of material preparation. This emission is reported to appear at 614 nm in GaN prepared by radio-frequency sputtering⁷ or at 611 nm by Hirata et al.¹² in GaN powder prepared by a combustion method. Hao et al.²¹ report this transition in Ga₂O₃ to occur at 617 nm while Kitai²² assigns ⁵D₀ → ⁷F₂ emission to a set of lines at 621 nm in Ga_{2-x-y}In_xEu_yO₃ thin-film devices. Well-known oxide phosphors of Y₂O₃:Eu, YVO₄:Eu and Y₂O₂S:Eu yield the dominant ⁵D₀ → ⁷F₂ emission at wavelengths of 612, 619, and 625 nm, respectively.

In our earlier study involving AlN:Eu³⁺ powders, the main transition was observed near 612 nm.¹³ Considering that the powder samples used in this study had higher oxygen impurity concentration compared to thin films grown epitaxially, it was assumed that Eu

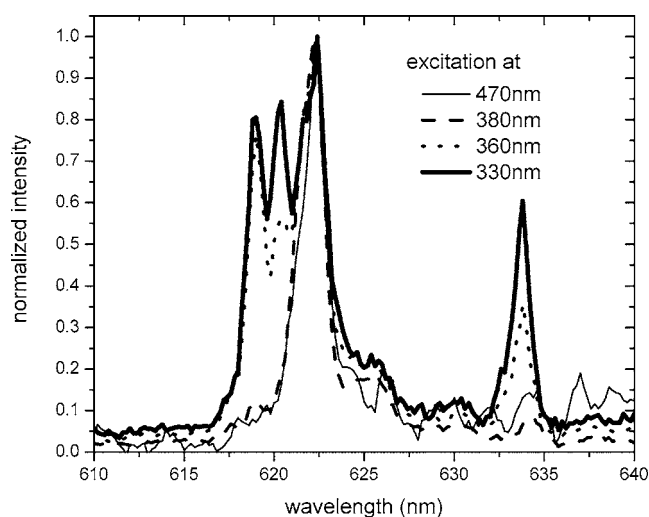


Figure 2. Main red emission lines of Eu^{3+} in GaN for lamp excitation at 330 nm (thick solid), 360 nm (dotted), 380 nm (dashed), and 471 nm (thin solid line).

ions segregate in the oxygen-rich regions. Only in high-purity powder samples of GaN grown directly from metal precursors has this transition been demonstrated near 621 nm.¹⁵

The $^5\text{D}_0 \rightarrow ^7\text{F}_2$ transition of Eu^{3+} is known to shift around in various host materials and is probably very dependent on the ligands. Observing the $^5\text{D}_0 \rightarrow ^7\text{F}_2$ transition around 621–622 nm in GaN is not entirely proof by itself for having Eu^{3+} ions incorporated into the nitride lattice. Yet, based on literature on thin films, it can be considered as a good indication that these ions are in a similar environment as in high-purity GaN powder or thin films. The other prominent lines in Fig. 1 have been attributed to $^5\text{D}_1 \rightarrow ^7\text{F}_4$ transition (at 634 nm) and to $^5\text{D}_0 \rightarrow ^7\text{F}_3$ transition (around 663–665 nm) of trivalent europium based on the data published in the literature.²³

More detailed luminescence in the red part of the spectrum is shown in Fig. 2 for low-excitation densities (Xe-lamp). Varying excitation wavelength yields multiple $^5\text{D}_0 \rightarrow ^7\text{F}_2$ hypersensitive peaks between 619 and 623 nm. Upon exciting into sharp excitonic absorption at 360 nm or above the bandedge at 330 nm, at least three (major) $^5\text{D}_0 \rightarrow ^7\text{F}_2$ lines at 619, 620.4, and 622.4 nm and one $^5\text{D}_1 \rightarrow ^7\text{F}_4$ emission at 633.8 nm are observed. On direct pumping at 470 nm through $^7\text{F}_0$ to $^5\text{D}_2$ transition of Eu^{3+} or at wavelengths between that and the excitonic absorption (for example, with 380 nm excitation), only a single $^5\text{D}_0 \rightarrow ^7\text{F}_2$ peak at 622.4 nm is recorded and no radiative relaxation from $^5\text{D}_1$ level at 633.8 nm is observed. This behavior is very similar to the one described by Nyein et al. in GaN:Eu under 471 nm resonant excitation.²⁴ It shows clearly the difference between charge carrier (or host-activator energy transfer) mediated and direct excitation of the activator ions.

As many as five peaks (some potentially unresolved) due to the $^5\text{D}_0 \rightarrow ^7\text{F}_2$ transition are observed in this work (Table I). Similar

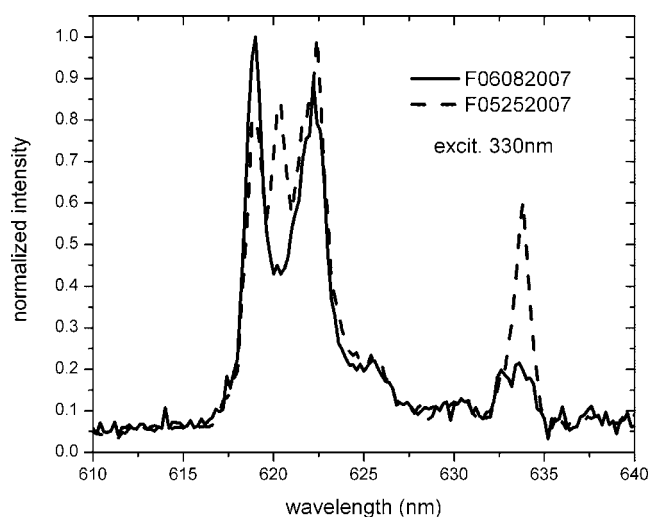


Figure 3. Comparison of emission spectra for two different GaN:Eu³⁺ films with different number of distinct $^5\text{D}_0 \rightarrow ^7\text{F}_0$ transition lines around 620 nm.

results for the $^5\text{D}_0 \rightarrow ^7\text{F}_2$ transitions have also been reported for GaN:Eu³⁺ films prepared by methods other than the MOVPE approach used in this work.^{23,25–27} Complete lifting of the orbital degeneracy due to low site symmetry could also result in five Stark-split lines. Thus, the occupancy of multiple activator sites cannot be established by the $^5\text{D}_0 \rightarrow ^7\text{F}_2$ transition alone. Nevertheless, we find additional support for different activator environments in Fig. 3. One of the two GaN:Eu films (F06082007) compared does not exhibit the 620.4 nm emission peak for the same 330 nm excitation. In this film, europium ions corresponding to $^5\text{D}_0 \rightarrow ^7\text{F}_2$ wavelength of 620.4 nm constitute at best a negligible minority. In order to confirm multiple sites by the spectral group of $^5\text{D}_0 \rightarrow ^7\text{F}_2$ transitions, the entire region up to ~ 700 nm was analyzed with higher resolution. The observed emission peaks are listed in Table I, along with their most likely assignments. Radiative decay from $^5\text{D}_0$ to $^7\text{F}_0$ involves nondegenerate levels that cannot be further split due to the crystal-field. This is a forbidden transition, yet it could occur at a very low symmetry site due to ligand field effects. The presence of multiple peaks instead of a single one in the region of $^5\text{D}_0 \rightarrow ^7\text{F}_2$ is a clear indication of europium ions in several different environments. As many as five sites have been found previously in the 570–590 nm wavelength interval of the same sample by Hömmerich et al.²³ who presented high-resolution PL excitation spectra locating peaks at 571, 585.8, 587.9, 588.9, and 589.4 nm at liquid helium temperatures in samples grown by MBE. Dierolf et al.²⁸ determine excitation wavelengths of 570.9, 584.6, 585.5, 587.9, 588.8, and 589.3 nm that can be associated with $^5\text{D}_0 \rightarrow ^7\text{F}_0$ transition. However, they argue that some of them are replicas due to coupling to phonons that reduce the number of distinct sites to four. Peng et al. report the same transitions at 591.9, 589.9, 588.5, and 585.2 nm.²⁷ We find this region to contain several lines (Table I), including a broader and probably unresolved transition at ~ 571 nm that may contain multiple components. However, it is not clear whether there could also be some contributions from $^5\text{D}_1 \rightarrow ^7\text{F}_3$ transitions.²⁹ These observations suggest that Eu^{3+} ions occupy multiple sites in the GaN films prepared by the MOVPE method in this study.

The most probable location for europium is a substitutional gallium site. Occupation of a Ga site by a rare-earth ion has been confirmed by extended X-ray absorption fine structure measurements.^{30,31} It has been speculated that interstitial sites near defects or impurities are responsible for more broadened, nonexponentially decaying $^5\text{D}_0 \rightarrow ^7\text{F}_0$ emission lines.²⁴ Also, some of these sites could be located in a secondary phase. However, considering the fact that the peaks between 619 and 623 nm have similar inten-

Table I. Observed emission peaks from Eu^{3+} in GaN.

Observed peaks (nm)	Spectroscopic assignment
571.0, 583.4, 585.7, 589.0, 591.5, 593.1, 595.0, 595.9	$^5\text{D}_0 \rightarrow ^7\text{F}_0$ ($^5\text{D}_1 \rightarrow ^7\text{F}_3$)
599.0, 601.0, 602.0, 605.4	$^5\text{D}_0 \rightarrow ^7\text{F}_1$
619.0, 620.4, 621.6, 622.4, 625.5	$^5\text{D}_0 \rightarrow ^7\text{F}_2$
633.8	$^5\text{D}_1 \rightarrow ^7\text{F}_4$
660.5, 663.0, 665.5	$^5\text{D}_0 \rightarrow ^7\text{F}_3$
717.5, 718.0	$^5\text{D}_0 \rightarrow ^7\text{F}_4$

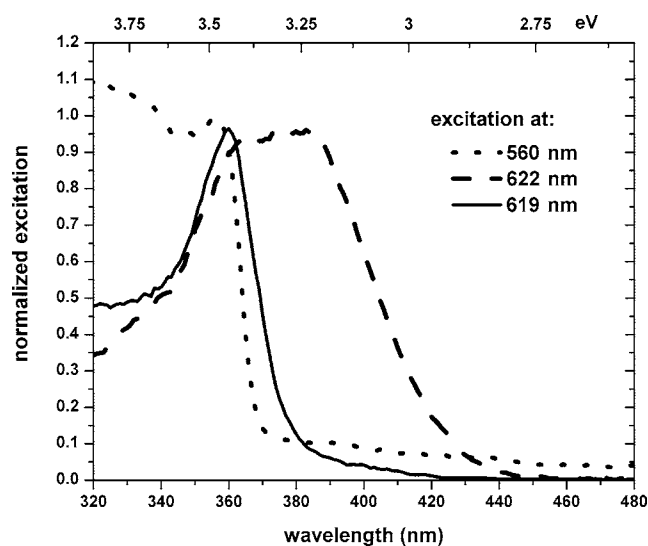


Figure 4. Excitation spectra corresponding to emission at 622 nm (dashed line) and 619 nm (solid line) due to Eu^{3+} . The excitation spectrum corresponding to defect emission at 560 nm (dotted line) is shown for comparison.

sities and that no secondary phase is indicated by XRD measurements, we believe that all the emitting sites are located in gallium nitride.

The PLE spectra for 619 and 622 nm emissions from the $^5\text{D}_0 \rightarrow ^7\text{F}_0$ transition of Eu^{3+} are shown in Fig. 4. We do not show the corresponding PLE spectrum for 620.4 nm emission because of the strong overlap this emission peak with that of 622 nm emission. For comparison, the excitation curve for emission near 560 nm due to lattice defects (most likely the defect center associated with the yellow band) is also presented. The PLE spectra for 619 and 622 nm emissions develop peaks near the bandedge of GaN. Most likely, these two emissions are associated with Eu^{3+} ions at two different sites. The excitation spectrum for the 619 nm emission from Eu^{3+} and that for the 560 nm emission from defects show a well-defined peak near 360 nm that can be attributed to absorption by the host, and subsequent emission via energy transfer from the host to the luminescent centers. This host-related excitation peak is not well resolved for 622 nm emission from Eu^{3+} . However, the similarity of the short wavelength tails of the excitation peaks for 619 and 622 nm clearly suggests that the broad excitation peak for 622 nm consists of a host-related peak similar to that of 619 nm emission and unresolved peak(s) associated with excitations below the band-edge. Because both the 619 and 622 nm emissions have PLE peaks near 360 nm, which corresponds to near the bandgap excitation of GaN, it is reasonable to conclude that the corresponding centers are located in GaN and are nonradiatively excited by energy transfer from the host. This excitation process is similar to the defect emission at 560 nm. The excitation spectrum for 622 nm emission exhibits another broadband that peaks near 400 nm below the band gap. This peak has been attributed to a charge transfer transition in nitride lattices.^{8,32,33} We tend to favor its assignment to a defect-related absorption for the following reasons.²⁵ The band is nearly nonexistent for the 619 nm excitation. Only a drastic change in metal-nitrogen distance could possibly push the charge transfer to such high energies that this band does not appear at excitation energies below the bandgap for one of the sites. It is possible that this band is associated with the broad but weak excitation peak for the defect emission at 560 nm (Fig. 4). Therefore, the excitation peak near 400 nm is most likely associated with some unidentified defect center located near Eu^{3+} ions that emit at 622 nm. Whether it is similar to that conjectured by Wang et al.²⁵ in comparison to the Er^{3+} centers in GaN³⁴ needs further careful investigation.

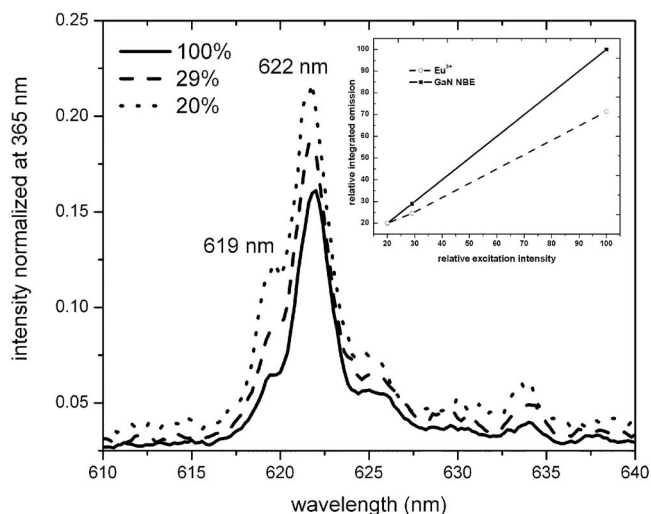


Figure 5. Excitation power dependent intensity of Eu^{3+} emission: a full laser output (estimated at $\sim 5 \text{ mJ/cm}^2$, solid line), and its reduction by 3.5 (dashed line) and 5 times (dotted line). The inset shows relative changes in integrated emission intensities as a function of excitation power (dashed line: Eu^{3+} emission).

On increasing the excitation energy, the excitation efficiency of europium ions is observed to decrease rapidly (Fig. 4). This behavior has often been observed in inorganic (powder) phosphors upon exciting the host lattice at energies higher than the bandgap.³⁵ It is usually explained in terms of increasing recombination of e-h pairs via surface states.³⁶ Radiation above the bandgap energy is absorbed closer to the film or particle surface due to rapidly increasing absorption coefficient and more free electrons or holes arrive at the surface before any radiative recombination in the bulk could take place. In contrast, the excitation efficiency for the yellow defect emission keeps on increasing monotonically with increasing excitation energy. It develops a peak near the bandedge but keeps on rising at higher energy. The likely explanation for this behavior is that the defect concentration near the surface is very high; thus, the radiative transition through defect states compete effectively with nonradiative transitions on the surface states.

The most significant conclusion from these measurements is that the europium ions are tightly coupled to the host lattice in the sense that excitation of Eu^{3+} ions occurs via nonradiative energy transfer from the host. Whether the exact mechanism is the Dexter-Forster type^{37,38} of energy transfer or recombination of itinerant electrons and holes at the Eu^{3+} sites needs to be investigated further.

In order to study the response of GaN: Eu^{3+} at higher excitation densities, laser excitation of 10 Hz/5 ns pulses was used. The excitation wavelength was chosen near the band-edge absorption energy (360 nm) which results in the generation of pairs with low kinetic energy (near the Γ point of the Brillouin zone) and approximately coincides with the effect of electrical excitation (e-h injection) before the recombination at activator ions occurs.

Our first observation is the reversal of peak intensities for GaN NBE at 365 nm and $^5\text{D}_0 \rightarrow ^7\text{F}_0$ transitions of Eu^{3+} compared to lamp excitation. This by itself constitutes a reduction in relative activator output of more than an order of magnitude. Figure 5 demonstrates changes in the $^5\text{D}_0 \rightarrow ^7\text{F}_0$ line intensities of Eu^{3+} from 610 to 640 nm for three incident excitation power values with $\sim 5 \text{ mJ/cm}^2$ per pulse as the maximum (instantaneous power of 1 MW/cm^2). The spectra have been normalized to 365 nm NBE intensities from GaN host (not shown) while the incident laser excitation is reduced by a factor of 3.5 and 5 using neutral density filters. One immediately notes the falling intensity of this red emission with respect to the NBE emission with increasing laser power. This behavior is further exemplified by the inset in Fig. 5, where the

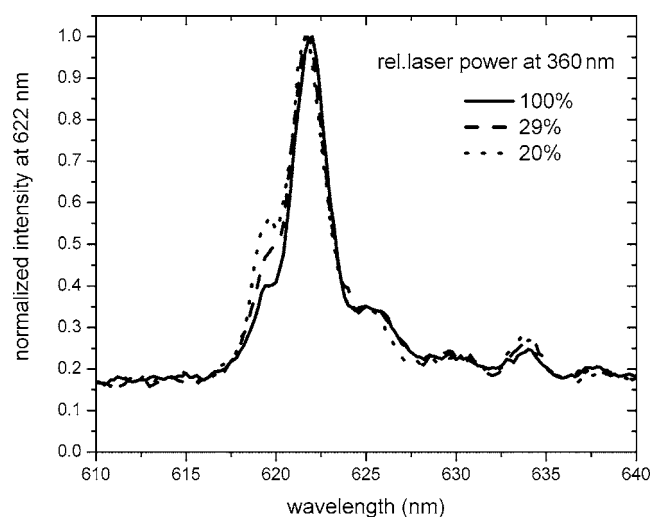


Figure 6. Excitation power-dependent intensity of Eu^{3+} emission (as in Fig. 5). The peak intensities for the three curves have been normalized at 622 nm.

intensities of the NBE and emission from the Eu^{3+} ions relative to the NBE emission at full laser power of 5 mJ/cm^2 per pulse are plotted against the input excitation intensity relative to the highest intensity. Therefore, the solid line representing the variation of relative NBE emission to relative excitation intensity has a unit slope. In contrast, the dashed line for the Eu^{3+} emission has a slope less than unity, indicative of nonavailability of activator ions in the ground state as the excitation intensity increases. This phenomenon is referred to as the depletion of ground state of the activator ions.³⁶ It foretells the possibility of eventual saturation of activator emission (i.e., development of a plateau in emission intensity vs excitation intensity curves) in rare-earth-doped materials for high exciton concentration with above the bandgap radiation.³⁶ In the present case, it is actually expected because both the density of recombination sites (on the order of 10^{20} cm^{-3} for the Eu activators compared to GaN lattice ions at 10^{22} cm^{-3}) and the excited state decay time (on the order of 10^{-9} s for excitonic emission vs $\sim 10^{-4} \text{ s}$ in the case of europium) are less favorable for the red emission compared to the NBE. We also note a nonuniformity in GaN:Eu output in response to the laser intensity change. In Fig. 6, the spectra have been normalized to the peak value of the red emission at 622 nm. Because the emission profile is assumed to consist of multiple contributions due to two or more types of europium ions in the GaN lattice, one finds the site giving rise to the 619 nm component to be slightly more sensitive to the excitation density increase as observed earlier by Bodious et al.³⁹ Assuming the same excitation efficiency for all the sites at 360 nm, the observed nonuniform response of various sites translates into higher population of the second type of europium ions that are capable of receiving their excitation through the defects. No attempt has been made in this work to extract excitation capture cross sections from the observed variation of the light output data.

Conclusion

In this paper, the spectroscopic characteristics of GaN:Eu³⁺ thin films deposited by the MOVPE method were reported in detail. The most significant aspect of our deposition process is that it was carried out at atmospheric pressure using a MOVPE reactor specifically designed for this purpose. Spectroscopically, the thin films are of similar quality compared to those reported by earlier workers. Emission from the Eu^{3+} ions occurred at $\sim 620 \text{ nm}$ due to ${}^5\text{D}_0 \rightarrow {}^7\text{F}_0$ transition, indicating that the activator ions are most likely located in the nitride lattice. The excitation spectra showed energy transfer from the host to the activator ions upon near the band-edge excitation.

Our results clearly support multiple-site occupancy of Eu^{3+} ions in GaN.²³⁻²⁷ The nature of the sites other than the substitutional site near the location of Ga ions is not well understood. In a recent work using first-principles methods, Mishra et al.⁴⁰ showed that Eu ions are thermodynamically stable at the Ga site. However, it is not clear what other sites are available in the GaN lattice that could accommodate the large rare-earth ions. The effect of multiple-site occupancy on the electrical properties of GaN thin films for device application needs further investigation, particularly from the structural point of view.

We also studied the dependence of Eu^{3+} emission intensity on increasing excitation density. The eventual saturation of emission could be a concern for operating devices at high current densities. However, our films are far from optimized. The observed sublinearly could be due to lateral inhomogeneity of distribution of activator ions and increasing absorption of radiation near the thin-film surface, which may not be a problem when the e-h pairs are uniformly distributed within the bulk. This issue needs to be studied further.

This work demonstrated the plausibility of using thin films of GaN doped with Eu^{3+} ions for converting directly the e-h pairs to red light within the device itself. Similar studies for generating green and possibly blue emission need to be explored using the MOVPE deposition process. Development of efficacious thin films of GaN-activated rare-earth ions capable of emitting in the red, green, and blue region of the visible spectrum could potentially improve the efficacy of the solid-state white-light sources.

Acknowledgments

We thank Dr. B. Han for many helpful discussions. This work was supported by grant no. DE-FC26-04NT42274 from the U.S. Department of Energy.

OSRAM SYLVANIA assisted in meeting the publication costs of this article.

References

1. A. J. Steckl and R. Birkhan, *Appl. Phys. Lett.*, **73**, 1700 (1998).
2. S. Morishima, T. Maruyama, M. Tanaka, Y. Masumoto, and K. Akimoto, *Phys. Status Solidi A*, **176**, 113 (1999).
3. H. J. Lozykowski, W. M. Jadwisnienczak, and I. Brown, *Appl. Phys. Lett.*, **74**, 1129 (1999).
4. A. J. Steckl, J. Heikenfeld, D. S. Lee, and M. Garter, *Mater. Sci. Eng., B*, **81**, 97 (2001).
5. J. B. Gruber, B. Zandi, H. J. Lozykowski, and W. M. Jadwisnienczak, *J. Appl. Phys.*, **92**, 5127 (2002).
6. W. M. Jadwisnienczak and H. J. Lozykowski, *Opt. Mater. (Amsterdam, Neth.)*, **23**, 175 (2003).
7. J. H. Kim and P. Holloway, *J. Appl. Phys.*, **95**, 4787 (2004).
8. J. Sawahata, H. Bang, J. Seo, and K. Akimoto, *Sci. Technol. Adv. Mater.*, **6**, 644 (2005).
9. H. Bang, S. Morishima, J. Sawahata, J. Seo, M. Takiguchi, M. Tsunemi, and K. Akimoto, *Appl. Phys. Lett.*, **85**, 227 (2004).
10. M. Pan and A. J. Steckl, *Appl. Phys. Lett.*, **83**, 9, 2003.
11. G. Blasse and B. C. Grabmaier, *Luminescent Materials*, Springer-Verlag, New York (1994).
12. G. A. Hirata, F. Ramos, R. Garcia, E. J. Bosze, J. McKittrick, O. Contreras, and F. A. Ponce, *Phys. Status Solidi A*, **188**, 179 (2001).
13. B. Han, K. C. Mishra, M. Raukas, K. Klinedinst, J. Tao, and J. Talbot, *J. Electrochem. Soc.*, **154**, J262 (2007).
14. B. Han, K. C. Mishra, M. Raukas, K. Klinedinst, J. Tao, and J. Talbot, *J. Electrochem. Soc.*, **154**, J44 (2007).
15. C. B. Poitras, H. Wu, A. C. Turner, M. G. Spencer, and M. Lipson, *Appl. Phys. Lett.*, **89**, 111912 (2006).
16. K. Hara, N. Ohtake, and K. Ishi, *Phys. Status Solidi B*, **216**, 625 (1999).
17. J. M. Zavada, S. X. Lin, N. Nepal, H. X. Jiang, J. Y. Lin, P. Chow, and H. Bertog, *Appl. Phys. Lett.*, **84**, 1061 (2004).
18. C. Ugolini, N. Nepal, J. Y. Lin, H. X. Jiang, and J. M. Zavada, *Appl. Phys. Lett.*, **89**, 151903 (2006).
19. M. A. Reschikov and H. Markoc, *J. Appl. Phys.*, **97**, 061301 (2005).
20. W. M. Jadwisnienczak, H. J. Lozykowski, I. Berishev, A. Bensaoula, and I. G. Brown, *J. Appl. Phys.*, **89**, 4384 (2001).
21. H. Hao, Z. D. Lou, I. Renaud, and M. Cocivera, *Thin Solid Films*, **467**, 182 (2004).
22. A. H. Kitai, *Thin Solid Films*, **445**, 367 (2003).
23. U. Hömmerich, E. E. Nyein, D. S. Lee, A. J. Steckl, and J. Zavada, *Mater. Sci. Eng., B*, **105**, 91 (2003).
24. E. E. Nyein, U. Hömmerich, J. Heikenfeld, D. S. Lee, A. J. Steckl, and J. Zavada, *Appl. Phys. Lett.*, **82**, 1655 (2003).

25. K. Wang, R. W. Martin, K. P. O'Donnel, V. Katchkanov, E. Nogales, K. Lorenz, E. Alves, S. Ruffenach, and O. Briot, *Appl. Phys. Lett.*, **87**, 112107 (2005).
26. T. Andreev, N. Q. Liem, Y. Hori, M. Tanaka, O. Oda, D. L. S. Dang, and B. Daudin, *Phys. Rev. B*, **73**, 195203 (2006).
27. H. Peng, C. Lee, H. O. Everitt, C. Munasinghe, D. S. Lee, and A. J. Steckl, *J. Appl. Phys.*, **102**, 073520 (2007).
28. V. Dierolf, Z. Fleischman, C. Sandmann, A. Wakahara, T. Fujiwara, C. Munasinghe, and A. Steckl, *Mater. Res. Soc. Symp. Proc.*, **866**, 73 (2005).
29. T. Monteiro, C. Boemare, M. J. Soares, R. A. Sa Ferreira, L. D. Carlo, K. Lorenz, R. Vianden, and E. Alves, *Physica B*, **308**, 22 (2001).
30. P. H. Citrin, P. A. Northrup, R. Birkhahn, and A. J. Steckl, *Appl. Phys. Lett.*, **76**, 2865 (2000).
31. H. Bang, S. Morishima, Z. Li, K. Akimoto, M. Nomura, and E. Yagi, *J. Cryst. Growth*, **237–239**, 1027 (2002).
32. M. Tanaka, S. Morishima, H. Bang, J. S. Ahn, T. Sekiguchi, and K. Akimoto, *Phys. Status Solidi C*, **0**, 2639 (2003).
33. P. Dorenbos and E. van der Kolk, *Appl. Phys. Lett.*, **89**, 061122 (2006).
34. S. Kim, S. J. Rhee, X. Li, J. J. Coleman, and S. G. Bishop, *Appl. Phys. Lett.*, **76**, 2403 (2000).
35. J. K. Berkowitz and J. A. Olsen, *J. Lumin.*, **50**, 111 (1990).
36. K. C. Mishra and M. Raukas, *J. Electrochem. Soc.*, **151**, H105 (2004).
37. T. Forster, *Naturwiss.*, **33**, 166 (1946).
38. D. L. Dexter, *J. Chem. Phys.*, **21**, 836 (1953).
39. L. Bodious, A. Oussif, A. Braud, J.-L. Doualan, R. Moncorgé, K. Lorenz, and E. Alves, *Opt. Mater. (Amsterdam, Neth.)*, **28**, 780 (2006).
40. K. C. Mishra, V. Eyert, and P. C. Schmidt, *Z. Phys. Chem.*, **221**, 1663 (2007).